An Analysis of Oxygen Absorption in a Tubular Membrane Oxygenator

R. G. BUCKLES, E. W. MERRILL, and E. R. GILLILAND

Massachusetts Institute of Technology, Cambridge, Massachusetts

An analysis of oxygen absorption by blood flowing through a small oxygen-permeable fiber in steady state laminar flow is presented. The rigidity and geometry of the fibers eliminate unpredictable shunting and distention, permitting a more detailed analysis of blood-membrane factors than has previously been undertaken. The mathematical analysis treats the blood as a homogeneous, non-Newtonian fluid with a reversible nonlinear oxygen sink (erythrocytes). The differential equations are solved numerically and the results of the parametric analysis are presented. The parameters that have a major influence on residence time necessary to obtain a specified oxygen content are the Grashof number, the concentration of hemoglobin in the blood, and wall Nusselt number, γ: $\gamma = D_L\alpha_L/D_M\alpha_M \ln [1 + t_m/R]$ where D = diffusion coefficient, α = Bunsen solubility coefficient, subscript L = liquid in tube, subscript M = tube material, R = inner radius of tube, t_m = tube wall thickness.

Comparison of the experimental results to the model indicate that mixing due to the heterogeneous nature of blood is minimal and that the major limitation in oxygen absorption is the blood film. Means of reducing this resistance are discussed.

An increasing number of surgical and research preparations require the temporary replacement of heart and lung function by mechanical devices. Gas exchange devices (inadequately described as *oxygenators*) are amenable to mass transfer analysis but are complicated due to the more complex blood-gas reaction and the heterogeneity of the blood. Although such an analysis is helpful in the development of any gas exchange device, the usual economic considerations that motivate an analysis of large equipment is not present in oxygenator design. Hence, oxygenators have been developed somewhat empirically.

However, recent studies have shown that significant irreversible lipoprotein denaturation occurs at the large blood-gas interfaces in existing devices; this limits the total time available for use of the oxygenator. A membrane oxygenator, in which the blood is separated from the gas by a highly permeable membrane, relieves this limitation by replacing the highly active liquid-gas surface with a moderately passive blood-membrane surface (*9*, *15*). Since such a device has an added impedance to mass transfer, its over-all size must be increased. When this requirement is coupled with the inability to mechanically produce a thin blood film between two thin membranes, the resulting device is quite large and cumbersome. In addition, it requires an excessive priming volume (priming volume/total body blood volume = 1) (*11*). Because these limitations have restricted the use of such devices, it is necessary to evaluate their performance from a more rigorous point of view.

In this paper an analysis is presented of the variables affecting oxygen absorption in an experimental membrane oxygenator. The emphasis is on an elucidation of the hydrodynamic and biochemical parameters, avoiding, in so far as possible, the artifacts in flow rate due to geometry variations and lack of structural rigidity. The parameters to be chosen represent as realistic a model as possible; approximations will be selected in order to yield a conservative estimate of oxygen uptake.

Figure 1 depicts an experimental micro-oxygenator in which the complications of variable flow patterns and membrane geometry have been eliminated. Blood is pumped at a steady rate through a hollow silicone rubber fiber, which is located in an oxygen-rich gas chamber. The amount of oxygen absorbed by the blood is measured with a Clark-type oxygen electrode that is sensitive to the oxygen partial pressure of blood. The fibers are formed with a constant inside diameter and exhibit a negligible distention when subjected to flow conditions. It is possible to obtain a pressure-insensitive fiber with a thin wall only if the fiber diameter is very small. The fiber is coated at the inlet with an impermeable epoxy for

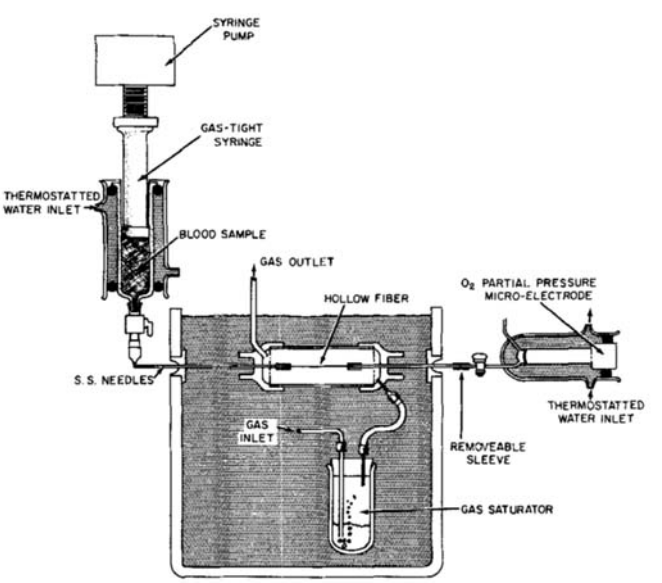

Fig. 1. Blood-gas exchange cell, schematic.

R. G. Buckles is at the National Naval Medical Center, Bethesda, Maryland.

greater than 100 diam. so that one may assume that the blood flows in a well-developed laminar profile along the gas exchange portion of the tube (*1*).

The absorption of oxygen into the blood is a multistep process involving diffusion and chemical reaction (*20*). Oxygen first diffuses radially through the silica filled silicone rubber; upon entering the blood, oxygen diffuses through the plasma both radially and toward the adjacent erythocytes. Diffusion to the erythocyte follows a concentration gradient established by the reaction of oxygen with hemoglobin within the cell. This hemoprotein has such a high affinity for oxygen that it extracts the gas from surrounding plasma and reacts with it in a reversible shared-bond complex (*20*). Oxygen reaching the erythrocyte surface diffuses through the membrane, then diffuses and reacts with the relatively stationary hemoglobin molecules within the erythrocyte. The equilibrium relationship between oxygen partial pressure and degree of oxygen binding to hemoglobin (percent saturation) is a sigmoid-shaped curve, reflecting the variations in oxygen affinity of the four oxygen binding sites (Figure 2). When all the hemoglobin within a red cell is saturated with oxygen (at a P_{O_2} of approximately 150 mm. mercury), oxygen may diffuse through the erythrocyte in a radial direction in parallel with diffusion through plasma.

Since Benis (*1*) has shown that blood in steady state laminar flow behaves like a homogeneous non-newtonian fluid, we may describe the velocity profile exactly. Since blood flows in the laminar regime, blood near the tube wall will be exposed to a longer residence time within the oxygenator than blood near the centerline. In any case, provided the flow is nonturbulent, the blood leaving the oxygenator will consist of a thin annulus of saturated blood adjacent to the wall and an inner core of partially saturated blood (blood is saturated when each hemoglobin molecule has reacted with four oxygen molecules). The arterial blood is well mixed in the exit line prior to measurement by the electrode.

MATHEMATICAL DESCRIPTION

A mathematical description of the oxygen uptake by the model oxygenator (Figure 1) has been developed. The assumptions are conservative, that is, any deviation from the model would result in enhanced oxygen absorption.

The steady state absorption process is idealized as follows:

1. isothermal and iso-P_{CO_2} conditions exist.
2. metabolic consumption of oxygen is negligible.
3. the velocity profile in the tube is given by Benis' integration of the Casson equation (*1*).
4. the hemoglobin inside the erythrocyte is everywhere in equilibrium with the plasma located at the same radial position.
5. diffusion through the fiber wall occurs in a radial direction only.
6. arial diffusion in the blood is negligible.
7. the external gas has a constant oxygen partial pressure, P_o.

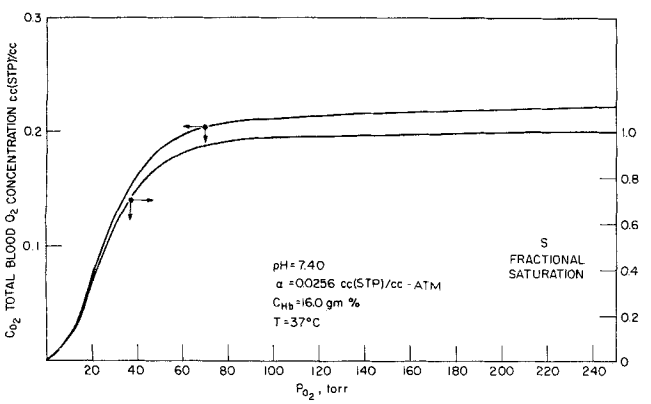

Fig. 2. Oxygen-hemoglobin equilibrium in normal whole human blood.

Incorporation of the preceding assumptions into a differential equation describing the steady state flux of oxygen in the liquid, and its boundary conditions, results in the following equations:

$$V(\rho)\left[\frac{\partial p}{\partial \chi}+\frac{\partial s}{\partial \chi}\right]=\frac{1}{\rho}\frac{\partial}{\partial \rho}\left(\rho\frac{\partial p}{\partial \rho}\right) \tag{1}$$

$$\text{At } \chi = 0, \quad \text{and any } \rho,\ p = p_i, \quad s = s_i(p_i) \tag{2}$$

$$\text{At } \rho = 1.0, \quad \text{and any } \chi, \quad \frac{\partial p}{\partial \rho}=\frac{1}{\gamma}(1-p) \tag{3}$$

$$\text{At } \rho = 0.0, \quad \text{and any } \chi, \quad \frac{\partial p}{\partial \rho}=0.0 \tag{4}$$

The velocity, $V(\rho)$, was given by Benis (*1*) as

$$V(\rho) = 1.0 \text{ when } \rho \leq \frac{\tau_y}{\tau_w} \tag{5}$$

$$V(\rho)=\frac{1}{K}\left[\frac{\tau_w}{2}(1-\rho^2)-\frac{4}{3}\tau_y(1-\rho^{3/2})+\tau_y(1-\rho)\right] \tag{6}$$

when $\rho > \tau_y/\tau_w$

where

$$K=\frac{\tau_w}{2}\left[1-\frac{\tau_y^2}{\tau_w}\right]-\frac{4}{3}(\tau_y\tau_w)^{1/2}\left[1-\frac{\tau_y^{3/2}}{\tau_w}\right]+\tau_y\left(1-\frac{\tau_y}{\tau_w}\right) \tag{7}$$

and, where p is the oxygen partial pressure (tension), s represents the oxygen carried by hemoglobin, γ is the wall-Nusselt number, and ρ and χ are the dimensionless radial and axial coordinates.

Equation (1) indicates that oxygen is transported axially by the physical movement of blood in two states: $V(\rho)\dfrac{\partial p}{\partial \chi}$ represents oxygen physically dissolved in the blood, while $V(\rho)\dfrac{\partial s}{\partial \chi}$ represents oxygen bound to hemoglobin. Under conditions of constant pH and P_{CO_2}, s is a function of p (*17*):

$$s=\frac{1{,}020\,C_{Hb}}{\alpha P_o}\left[\frac{\left(\frac{1+kP_op}{kP_op}\right)^3+m-1}{\left(\frac{1+kP_op}{kP_op}\right)^4+m-1}\right] \tag{8}$$

where k and m are empirically determined from the oxygen-hemoglobin equilibrium relationship and P_o is the gas phase oxygen tension.

Figure 2 presents this equilibrium expression for normal whole blood at 38°C. This figure also presents the curve for total oxygen concentration as a function of p; the total concentration is merely the sum of the oxygen dissolved (αP) and that bound to hemoglobin ($1.34 \cdot C_{Hb} \cdot s$).

The curve is shifted to the right under conditions of increased acidity (the Bohr effect) and increased temperature.

Because of the present controversy over the choice of an adequate thermodynamic model of the oxygen hemoglobin equilibrium, Equation (8) is isolated as a subroutine in the computer program and can be replaced by more suitable analytic expressions as they become available.

Equations (1) to (8) have been numerically solved on an IBM 7094 digital computer using the Crank-Nicolson finite difference method. Standard criteria for convergence and stability (*13*) were met by proper selection of time and space coordinates.

RESULTS OF THE MATHEMATICAL MODEL

The mathematical program is written so that experimental conditions may be input directly. The program and a sample problem are presented elsewhere (*4*). The computer output are tables of average P_{O_2}, ΔP, C_{O_2}, and both the average and local mass transfer coefficients, tabulated at selected values of χ.

Absorption Without Chemical Reaction

An extension of the classic Graetz problem (*12*) is obtained when $C_{Hb} = 0$ and $\tau_y = 0$. Under these conditions, the fluid exhibits newtonian properties and is subject to Henry's Law; and the dimensionless axial location, χ, is:

$$\left[\chi = \frac{x}{R} (N_{Re} N_{Sh})^{-1} = \frac{\pi}{2} N_{Gr} \right]$$

Since Equation (1) is reduced to a linear differential equation when reaction is neglected, the oxygen pressure is a function of the two coordinates and the constant, γ. If one computes the radially average tension, $p(\chi)$, the overall gas exchange can be expressed as

$$\Delta P = \frac{p(\chi) - p_i}{1 - p_i} = f(\chi, \gamma) \qquad (9)$$

The numerical solution of Equation (9) is presented in Figure 3. The exact Graetz solution (*12*) and the Leveque approximation (*16*) are presented for comparison with the case where $\gamma = 0.0$. At low values of ΔP, the accurate solution of the Graetz equation requires an excessive number of exponential terms; in this case the Leveque approximation (that is, treating the diffusion field as a flat plate of area $2\pi R$) is more accurate. The numerical solution is in agreement with these two analytical expressions at low and high values of ΔP. The numerical results for $\gamma = 2$ and $\gamma = 0.25$ coincide with the linearly interpolated curves from the data in Figure 2, of reference 22.

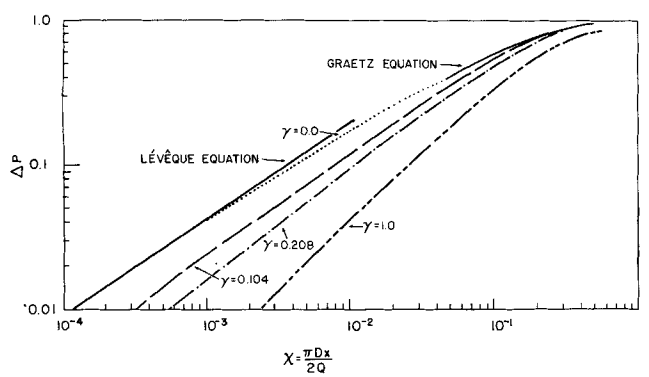

Fig. 3. Steady state mass transfer in a Newtonian liquid flowing inside a tube of finite mass transfer resistance.

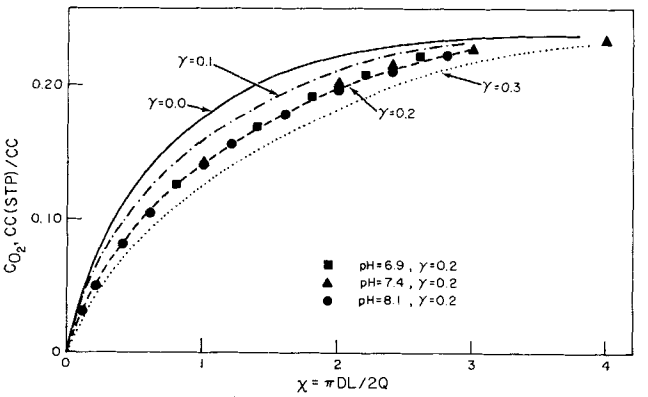

Fig. 4. Influence of membrane resistance on C_{O_2}. This figure presents the variation in oxygen uptake (C_{O_2}) as a function of the Graetz number for different values of wall resistance. The influence of pH is also shown, when $\gamma = 0.2$. Blood characteristics: $m = 100$, $\alpha = 0.0256$ cc.(STP)/cc.-atm., $C_{Hb} = 16.0$ g.%. Operating parameters: parabolic velocity profile: $P_o = 760$ mm. mercury, $T = 38$°C.

Absorption And Chemical Reaction

When hemoglobin reacts with oxygen, a large variety of parameters are required. Inspection of Equations (1), (3), (6), and (8) indicate that the oxygen partial pressure depends on seven dimensionless parameters: χ, ρ, γ, τ_y/τ_w, $C_{Hb}/\alpha P_o$, kP_o, and m. Since the blood leaving the oxygenator is well mixed in the header, we consider only the radially-averaged partial pressure. Parametric studies showed that the velocity profile that results in the smallest gas exchange rate is the parabolic velocity profile. Since $\tau_y << \tau_w$ in most of our studies, the use of a parabolic profile is justified. Thus, the important parameters are χ, γ, $C_{Hb}/\alpha P_o$ and kP_o and m. The last two parameters define the oxygen-hemoglobin equilibrium line, and are therefore a function of pH, P_{CO_2}, and temperature.

Figure 4 presents the dependence of C_{O_2}, on the Graetz Number, χ, for different values of wall resistance, γ. Typical blood parameters are chosen at 38°C. (where a particular parameter is unknown, equivalent data for pure water is substituted). The inlet blood is fully reduced, and the gas in the surrounding gas space is pure oxygen at 760 mm. mercury pressure.

Figure 4 also presents curves computed for blood of different pH, all other parameters being held constant.

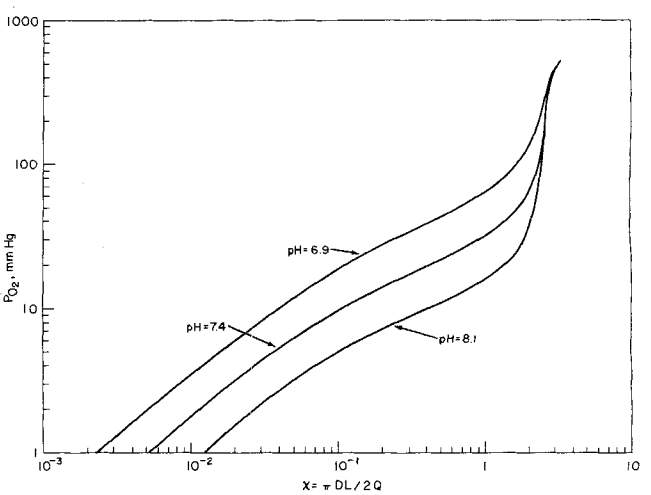

Fig. 5. Influence of pH on average P_{O_2}. This figure presents the average P_{O_2} in blood as a function of the Graetz number for cases in which a significant shift occurs in the oxyhemoglobin dissociation curve. Blood characteristics: $m = 100$, $\alpha = 0.0256$ cc.(STP)/cc.-atm., $D = 3.45 \times 10^{-5}$ sq.cm./sec., and $C_{Hb} = 16.0$ g. %. Operating parameters: parabolic velocity profile: $T = 38$°C., $\gamma = 0.2$, and $P_o = 760$ mm. mercury.

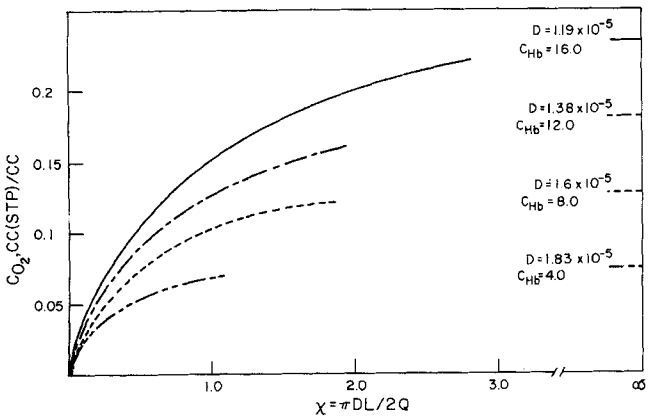

Fig. 6. Influence of C_{Hb} on C_{O_2}. This figure presents the variation in oxygen uptake (C_{O_2}) as a function of the Graetz number for four different hemoglobin levels. Blood characteristics: α = 0.0213 cc.(STP)/cc.-atm., m = 125, K = 0.01084 mm. mercury^{-1}. Operating parameters: parabolic velocity profile: P_o = 760 mm. mercury, P_m = 6.16 × 10^{-8} cc.(STP)-cm./sq.cm.-sec.-cm. mercury, T = 38°C.

Figure 5 presents the influence of pH on the average arterial blood P_{O_2} as a function of χ for these same three samples (γ = 0.2).

The range represents about the maximum variation clinically observed. Comparison of Figures 4 and 5 show a large pH-dependent variation in arterial P_{O_2} (at a given value of χ) yet practically no variation in the amount of oxygen absorbed (C_{O_2}). Analysis of Figure 4 shows that $\frac{1}{\chi}\frac{\partial \chi}{\partial \gamma} = 2.5$ at most values of C_{O_2}. Thus, when γ = 0.1 (typical value) the wall resistance increases the overall contact time requirement about 25% over the value for γ = 0.0.

Figure 6 depicts the dependence of C_{O_2} on the hemoglobin concentration. The oxygen diffusivity is a function of hemoglobin levels, and will be discussed. The wall resistance was maintained constant throughout, although γ does vary for each curve due to the variations in D. There is a significant dependence of χ on the hemoglobin concentration at less than full saturation.

APPARATUS AND PROCEDURE

An experimental gas exchange cell was constructed to test the assumptions of the model given in the preceding section. In particular, the assumption of laminar flow in a heterogeneous fluid deserves some investigation. If the erythrocytes exhibit extensive collision interaction in the shear field, the model may be deemed altogether too conservative to be of any value.

The apparatus (Figure 1) consisted of a Harvard constant speed syringe pump, Hamilton gas tight syringes, stainless steel inlet and exit lines, and a Radiometer Type E5046 P_{O_2} electrode. The electrode signal is detected by a Radiometer 27 SEGM combination pH-P_{O_2}-P_{CO_2} meter. The inlet lines and gas exchange cell were immersed in a thermostatted lucite bath (Heta-thermo-regulator) and water was circulated from the bath to both the blood supply and the P_{O_2} electrode. The hollow fibers were of two sizes: (a) large silicone rubber fibers (0.0305 cm. I.D. × 0.0636 cm. O.D.) were made of Silastic® Medical Grade silicone rubber; (b) small fibers (0.00915 cm. I.D.) were made in our laboratory from RTV Silastic® Medical Adhesive.

Whole human blood (< 2 days old), anticoagulated with either ACD or heparin, was prepared according to standard procedures (*6*). It was tonometered with nitrogen (or nitrogen + 5% carbon dioxide) for greater than 1 hr. in a thermostatted tonometer to assure complete removal of oxygen and equilibration with carbon dioxide. After anaerobic transfer of the blood to the gas-tight syringe (including a small magnetic stirrer to avoid erythrocyte settling) the blood was pumped at a steady rate (± 0.1%) through the fiber and into the P_{O_2} electrode cuvette. The gas (pure oxygen, or 95% oxygen and 5% carbon dioxide) was saturated with water vapor and continuously passed through the gas exchange cell at ambient pressure.

The diffusivity of oxygen through water, plasma, and blood was determined by use of the numerical solution presented in the preceding section. If one uses blood that has been equilibrated with oxygen at a high P_{O_2} (see Figure 2), the hemoglobin is fully saturated and oxygen merely dissolves in the blood according to Henry's law. For these studies blood was equilibrated with air and the gas was pure oxygen. Determination of D is an iterative computation, described in detail in (*4*). The diffusivity in whole blood (D_{WB}) under these conditions includes the effect of diffusion through the erythrocyte.

RESULTS

The mathematical model is compared with data for distilled water at 38°C. in Figure 7. The oxygen solubility and diffusivity in water were obtained from standard references (*13*, *19*) and the corresponding data for the silicone rubber fiber was obtained in separate experiments (*4*).

By using the experimental results for plasma and water in the same fiber and the numerical solution, we have determined that the ratio of diffusivity in plasma to that in water is 0.5235 ± 0.152 [when α_p/α_w = 0.9 (*23*)].

By using fully saturated blood (H = 28%), the ratio of diffusivity in blood to that in distilled water was determined to be 0.387 ± 0.061. Therefore, the ratio of D_{WB}/D_p = 0.74.

In all cases, ΔP decreased as the flow rate increased in a given fiber. Preliminary studies showed that the use of plastic exit tubes resulted in considerable loss of oxygen by diffusion through the wall; although the permeability of these tubes is lower than silicone rubber, the liquid residence time is sufficiently long to permit a significant oxygen loss. The fiber position did not influence the results with whole blood. Even continual tapping of the fiber with a glass rod did not significantly alter the rate of oxygen absorption by whole blood.

Figure 8 presents the results of oxygen absorption by fully reduced whole blood, equilibrated with 5% carbon dioxide and 95% nitrogen. The curve was computed from experimental data on the blood used in the absorption studies. Although the figure ordinates are actually the experimental parameters measured, the computed curve requires further data on the equilibrium relationship between P_{O_2} and C_{O_2}. This information was obtained by the use of a dissociation curve analyzer (*4*).

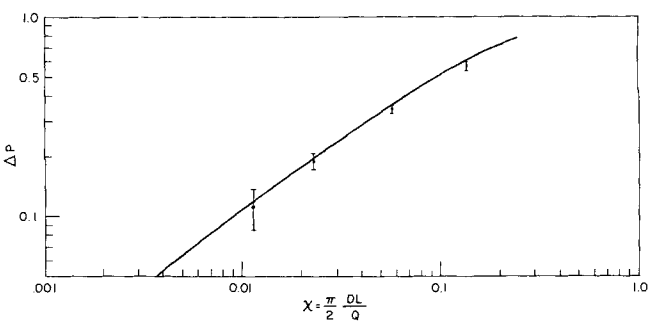

Fig. 7. Experimental data for oxygen absorption by water at 38°C. The curve was computed from Equations (1) through (8) from the following parameters: D = 3.56 × 10^{-5} sq.cm./sec. (*19*); α = 0.0236 cc.(STP)/cc.-atm. (*13*); the fiber length was 3.7 cm., and was 0.0636 cm. O.D.

® Registered trademark of Dow Corning, Inc., Midland, Michigan.

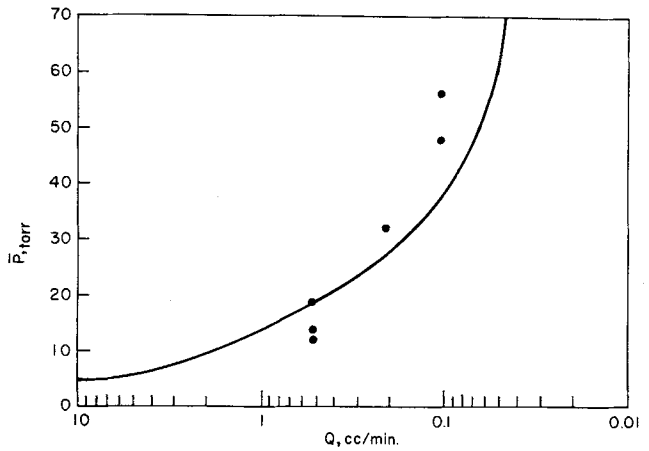

Fig 8. The influence of flow rate on oxygen absorption by whole reduced blood. Experimental conditions are: pH = 7.14, T = 38°C., C_{Hb} = 0.091, α = 0.0262, m = 125, K = 0.01084, D_m = 2.025 × 10^{-5}, α_m = 2.776 × 10^{-4}, P_o = 686, D_{WB} = 1.38 × 10^{-5}, X = 39.5. The solid curve was computed from the numerical solution to Equations (1) through (8).

DISCUSSION

Even though it was possible to build an experimental cell in which many of the mathematical assumptions could be attained, practical oxygenators seldom meet these restrictions. Heterogeneous fluids provide many mathematical complications, but biological fluids attain a higher order of complexity due to the synergistic cooperation of variables. Thus, as oxygen is absorbed by hemoglobin, the blood pH changes, due to the more acidic nature of oxyhemoglobin. From Figure 5 one can estimate that the computed iso-pH curve in Figure 8 is about 5% too low at P_{O_2} = 100 torr. In real oxygenators, the simultaneous removal of carbon dioxide actually increases the rate of oxygen absorption (*20*); this effect is only partly due to pH effects.

Metabolic oxygen consumption rates were quite noticeable when using fully saturated blood (in the determination of D_{WB}). During a 20 min. sequence of runs, the P_{O_2} of the blood in the syringe would drop over 10%. A linear interpolation was used to estimate the blood P_{O_2} before each run in the sequence.

The use of Benis' equation for the velocity profile in a non-newtonian fluid that exhibits a yield shear stress is the most conservative assumption in the mathematical model. The equation is based on the finding that Casson's model (*5*) does empirically correlate the rheological data for whole blood; Benis' model is then an integration of the Navier-Stokes equation for steady laminar flow in a round tube, incorporating the Casson equation for the viscosity. Benis showed that the equation correlated blood flow-pressure drop data for a wide variety of tube diameters (> 50μ I.D.) and materials. Although high speed cinemicrography has revealed movement of red cells in a random manner due to particle collisions, Benis' results suggest that this movement is not dynamically significant. The high volume fraction of erythrocytes in normal blood (v_{RBC} = 0.45) also precludes axial streaming to any great extent. Under conditions of reduced hematocrit, erythrocyte interaction may well enhance the oxygen absorption rate. Cokelet (*6*) has shown that the apparent newtonian viscosity of blood decreases dramatically below a hematocrit of 25%, presumably due to enhanced momentum transport near the wall.

Because of the uncertainty about mixing due to random erythrocyte motion and interaction, several runs at high flow rate were undertaken. Under this condition of large shear gradient the oxygen absorption is limited to the region near the wall and should be a sensitive detector of convective patterns. Figure 8 indicates that this model exhibits the closest agreement to experimental results in this region of high flow rate. Experiments at lower wall shear rates in very short fibers were not undertaken. It is therefore difficult to extrapolate our findings for oxygenators wherein a large change in bulk concentration occurs to the case of artificial kidneys.

The oxygen diffusivity determinations lend further support to the proposition that erythrocyte collisions do not significantly enhance oxygen absorption. The ratio D_p/D_W is predictable, within experimental error, by the simple Einstein equation D_p/D_W:η_W/η_p; and the ratio of D_{WB}/D_p is that ratio predicted from the classic equation of Fricke (*10*) for diffusivity through heterogeneous media with two characteristic diffusivities. The constants used to predict D_{WB}/D_p are: hematocrit, D_p = 1.86 × 10^{-5}, and D_{RBC} = 0.427 × 10^{-5} (*24*). It appears, therefore, that erythrocyte mixing, as a physiological phenomenon, does not occur to any great extent in vessels larger than 90μ I.D.

The assumption of instantaneous equilibration between an erythrocyte interior and the plasma at its surface is not conservative. To test the assumption, one can treat the oxygen-hemoglobin reaction as first-order, based on the P_{O_2} at the erythrocyte surface (*20*). The rate of mass transfer from the bulk plasma to the erythrocyte surface can be expressed by a flow-independent mass transfer coefficient (*21*). Where these two series processes were combined, taking into account the mean erythrocyte surface area (*4*), an over-all pseudo-first-order rate constant for oxygen removal from plasma was obtained. Danckwert's solution for radial diffusion accompanied by a first-order irreversible reaction (*7*) was then used to assess the importance of the reaction rate. It was found that the reaction rate so determined is several orders of magnitude greater than the diffusion parameters, justifying the assumption of an indefinitely fast reaction between oxygen and hemoglobin.

Axial diffusion in a liquid in laminar flow is generally negligible (*2*). This assumption is justified if the term $D\dfrac{\partial^2 C}{\partial x^2}$ is insignificant in comparison to the axial convection term, $v(r)\dfrac{\partial C}{\partial x}$ [this corresponds to the left hand side of Equation (1)]. Under experimental conditions, where L/R exceeds 1,000 and Q/RD exceeds 10,000, the axial diffusion term is 10^7 times smaller than the axial convection term.

On the other hand, axial diffusion in the wall could occur due to the large ratio of tube O.D. to I.D. Under extreme conditions, we estimate that axial diffusion in the rubber represents only 5% of radial diffusion. This would represent a very small increase in absorption rate at high flow rates.

An alternate analysis of oxygen absorption is the moving front concept of Thews (*24*). The blood is treated as two regions separated by a radially moving front. Outside the front, the blood is saturated, while the rest of the blood is reduced. Oxygen diffuses through the saturated blood to the interface where it reacts with the unsaturated hemoglobin. This concept has been extended to the present case where the gas first traverses a membrane, then diffuses through blood that is flowing with a parabolic velocity profile. The model neglects the oxygen that is physically dissolved and treats the oxygen tension at the interface as zero. The model indicates that the fiber length required to fully saturate the hemoglobin is given by

$$X = \frac{1020\, C_{Hb}}{\alpha\, P_G}\,[0.1875 + 0.25\gamma] \qquad (10)$$

Because of the two assumptions given above, the model is not a conservative estimate of the fiber requirement. For example, in Figure 8, the moving front model predicts complete saturation ($\overline{P}_{O_2} = 150$ torr) at $Q = 0.4$ cc./min. Actually, it requires $Q = 0.034$ cc./min.

Several design possibilities have become apparent from this study. They are predicated on the assumption that the liquid film absorption rate controls the process. That this is so may be seen in Figure 3 where the curve for $\gamma = 0.1$ (a typical experimental value) closely approximates the solution for $\gamma = 0.0$ (negligible wall resistance case). The numerical solution for the more complex reaction case indicated the same minimal dependence on wall resistance.

Therefore, any design that minimizes the liquid film resistance will significantly enhance the exchange rate. Elements placed in the blood stream which promote circulation of blood from the center to the walls have been shown to significantly reduce the size requirements of flat plate oxygenators (3). Periodic remixing (as in headers) will significantly enhance oxygen absorption. By using the model presented in this paper, it has been shown that the incorporation of two mixing zones reduces the overall exchanger length by 25%. In any case, one should strive for the thinnest blood film thickness feasible.

Paradoxically, one could easily use a much thicker silicone rubber membrane in many oxygenators and still enhance oxygen absorption rates. This is because the membrane serves mainly to contain the blood and provide mechanical support. In flat plate membrane oxygenators, as well as thin-walled tubular oxygenators, increased flow rates distend membranes, yielding considerable shunting and increased blood film thickness (*18.*) Thicker membranes would reduce distension and permit more shunt-free design. In addition, thicker membranes are safer. A particular advantage of the tubular oxygen absorber is the relatively small dependence of the wall resistance on the wall thickness; Equation (2) shows that γ depends on the log of $(R + t_m)/R$, rather than a linear dependence, as in flat membranes. Further, for a given pressure and membrane thickness, a tubular exchanger distends much less than a supported flat plate design (*4*).

NOTATION

C_{O_2} = total oxygen concentration in the liquid, cc. (STP)/cc.
C_{Hb} = hemoglobin concentration, g./cc.
D = oxygen diffusivity in the liquid phase; sq.cm./sec. (represents the over-all effective diffusivity through heterogeneous liquids)
D_M = oxygen diffusivity in the tube material, sq.cm./sec.
H = hematocrit, the volume fraction erythrocytes
k,m = empiric equilibrium constants used to describe the relation between P_{O_2} and C_{O_2} [Equation (8)]
N_{Gr} = Graetz Number, $= Dx/Q$
$p(\rho,\chi)$ = dimensionless oxygen partial pressure: $= P_{O_2}(\rho, \chi)/P_o$
$P_{O_2}(\rho,\chi)$ = partial pressure of dissolved (and reacted) oxygen as a function of ρ and χ, torr.
P_o = partial pressure of oxygen in gas space surrounding the rubber tube, torr.
Q = liquid flow rate; cc./sec.
r = radial coordinate; cm.
R = inside radius of rubber tube
$s(\rho,\chi)$ = dimensionless concentration of oxygen bound hemoglobin
t_m = tube wall thickness, cm.
$v(\rho)$ = axial velocity as a function of ρ, cm./sec.
v_{max} = maximum axial velocity, cm./sec.
$V(\rho)$ = dimensionless linear velicity as a function of ρ, $= v(\rho)/v_{max}$
x = axial distance from tube inlet; cm.
α = oxygen solubility constant in the liquid phase; cc. (STP)/cc.-atm.
α_M = Bunsen solubility coefficient in the tube material; cc. (STP)/cc.-atm.
γ = dimensionless tube wall resistance;
$$= \frac{D\,\alpha \ln \dfrac{R + t_m}{R}}{D_M \alpha_M}$$
χ = modified Graetz number,
$$= \frac{Dx}{R^2\, v_{max}} = \frac{\pi}{2} N_{Gr} = \frac{x}{R}\,(N_{Re} N_{Sh})^{-1}$$
ρ = dimensionless radius, $= r/R$
τ_y = yield shear stress of blood (*6*), dynes/cm.
τ_w = shear stress at the wall, dynes/cm.

Subscripts

P = plasma
WB = whole blood
DW = distilled water

LITERATURE CITED

1. Benis, A. M., Sc. D. thesis, Mass. Inst. Tech., Cambridge, Mass. (1964).
2. Bird, R. B., W. E. Stewart, and E. N. Lightfoot, "Transport Phenomena," John Wiley, New York (1960).
3. Bramson, M. L., J. J. Osborn, F. B. Main, M. F. O'Brien, J. S. Wright, and F. Gerbode, *J. Thor. Cardiovas. Surg.*, **50**, 391 (1965).
4. Buckles, R. G., Ph.D. thesis Mass. Inst. Tech., Cambridge, Mass. (1966).
5. Casson, N., "Rheology of Disperse Systems," Chapter 5, ed., C. C. Mill, Pergamon Press, New York (1959).
6. Cokelet, G. R., Sc.D. thesis, Mass. Inst. Tech., Cambridge, Mass. (1963).
7. Danckwerts, P. V., *Trans. Faraday Soc.*, **47**, 1013 (1951).
8. Davenport, H. W., "The ABC of Acid-Base Chemistry," Univ. of Chicago Press, Illinois (1958).
9. Dobell, A. R. C., M. Mitri, R. Galva, E. Sarkozy, and D. R. Murphy, *Ann. Surg.*, **161**, 617 (1965).
10. Fricke, H., *Physical Rev.*, **24**, 575 (1924).
11. Galletti, P. M., and G. A. Brecher, "Heart-Lung Bypass . . . Principles and Techniques of Extracorporeal Circulation," Grune and Stratton, New York (1962).
12. Graetz, L., *Ann. Phys.*, **18**, 79 (1883).
13. Hildebrand, F. B., "Introduction to Numerical Analysis," McGraw-Hill, New York (1956).
14. Hodgman, C. D., (ed.), "Handbook of Chemistry and Physics, 35th Ed.," Chem. Rubber Pub. Co., Cleveland, Ohio (1953).
15. Lee, W. H., Jr., D. Krumhaar, G. Derry, D. Sachs, S. H. Lawrence, G. H. A. Clowes, and J. V. Maloney, Jr., *Surg. Forum*, **12**, 200 (1961).
16. Lévêque, *Ann. mines*, [*Ser. 12*], **13**, 201, 305, 381 (1928).
17. Margaria, R., *Clin. Chem.*, **9**, 745 (1963).
18. Pierce, E. C., II, *J. Thor. Cardiovas. Surg.*, **39**, 438 (1960).
19. Reid, R. C., and T. K. Sherwood, "The Properties of Gases and Liquids," McGraw-Hill, New York (1958).
20. Roughton, F. J. W., *Brit. Med. Bull.*, **19**, 80 (1963b).
21. Satterfield, C. N., and T. K. Sherwood, "The Role of Diffusion in Catalysis," Mass. Inst. Tech., course notes (1963).
22. Schenk, J., and J. M. Dumoré, *Appl. Sci. Res.*, **4A**, 39 (1952).
23. Sendroy, J., Jr., R. T. Dillion, and D. D. Van Slyke, *J. of Biol. Chem.*, **105**(3), 597 (1935).
24. Thews, G., *Pflügers Archiv.*, **265**, 138 (1957).

Manuscript received June 16, 1967; revision received November 8, 1967; paper accepted November 9, 1967.